Control of Actin Polymerization in Live and Permeabilized Fibroblasts

Marc H. Symons and Tim J. Mitchison

Department of Pharmacology, University of California, San Francisco, California 94143

Abstract. We have investigated the spatial control of actin polymerization in fibroblasts using rhodamine-labeled muscle actin in; (*a*) microinjection experiments to follow actin dynamics in intact cells, and (*b*) incubation with permeabilized cells to study incorporation sites.

Rhodamine-actin was microinjected into NIH-3T3 cells which were then fixed and stained with fluorescein-phalloidin to visualize total actin filaments. The incorporation of newly polymerized actin was assayed using rhodamine/fluorescein ratio-imaging. The results indicated initial incorporation of the injected actin near the tip and subsequent transport towards the base of lamellipodia at rates >4.5 μm/min. Furthermore, both fluorescein- and rhodamine-intensity profiles across lamellipodia revealed a decreasing density of actin filaments from tip to base. From this observation and the presence of centripetal flux of polymerized actin we infer that the actin cytoskeleton partially disassembles before it reaches the base of the lamellipodium.

In permeabilized cells we found that, in agreement with the injection studies, rhodamine-actin incorporated predominantly in a narrow strip of <1-μm wide, located at the tip of lamellipodia. The critical concentration for the rhodamine-actin incorporation (0.15 μM) and its inhibition by CapZ, a barbed-end capping protein, indicated that the nucleation sites for actin polymerization most likely consist of free barbed ends of actin filaments. Because any potential monomer-sequestering system is bypassed by addition of exogenous rhodamine-actin to the permeabilized cells, these observations indicate that the localization of actin incorporation in intact cells is determined, at least in part, by the presence of specific elongation and/or nucleation sites at the tips of lamellipodia and not solely by localized desequestration of subunits. We propose that the availability of the incorporation sites at the tips of lamellipodia is because of capping activities which preferentially inhibit barbed-end incorporation elsewhere in the cell, but leave barbed ends at the tips of lamellipodia free to add subunits.

THE actin cytoskeleton is for a large part responsible for cell morphology and locomotion. It is composed of microfilaments together with a large series of actin binding proteins (Pollard and Cooper, 1986; Stossel et al., 1985) and displays many characteristic structures, which include stress fibers, lamellipodia and filipodia, and the cortical actin meshwork (Small, 1988). In a variety of cell types studied, a fast turnover has been observed between the microfilaments and the actin monomer pool (Condeelis et al., 1988; Glacy, 1983; Kreis et al., 1982; Omann et al., 1987). Although this turnover has been implicated in various aspects of cell behavior such as cell locomotion, cell spreading, and cell-cell contact (Buendia et al., 1990; Letourneau et al., 1987; Southwick et al., 1989), the exact nature and regulation of the actin polymerization-depolymerization activity underlying these phenomena is not yet known.

Actin dynamics in lamellipodia of fibroblasts and neuronal growth cones recently has gained attention, especially in relation to cell translocation (for reviews see Mitchison and Kirschner, 1988; Smith, 1988). Multiple lines of evidence suggest that actin polymerizes at the tips of lamellipodia and subsequently is transported in a centripetal fashion. The underlying molecular mechanisms of these phenomena are still poorly understood however, one problem being the lack of experimental systems in which to address the mechanism of spatial regulation. Furthermore, the rates of centripetal transport inferred from experimental studies using different methodologies have varied greatly, from <1 μm/min to >10 μm/min (Fisher et al., 1988; Forscher and Smith, 1988; Svitkina et al., 1986; Wang, 1985). It is currently difficult to determine whether this variation reflects differences in actin dynamics in the different systems or artifacts of the different techniques used.

It is generally thought that the regulation of actin polymerization involves sequestering of monomeric actin, effectively decreasing the free monomer concentration to a value close to the critical concentration for barbed-end incorporation, ~0.1 μM (Sanders and Wang, 1990; Stossel, 1989). In this framework, spatial control of actin polymerization would be exerted by local release of actin monomers, which could then either nucleate new filaments or incorporate into existing filaments. Capping of filaments could in principle provide an additional mechanism for the regulation of actin polymerization, but so far no experimental evidence has been obtained

to support this. In this paper we present results which strongly suggest that spatially regulated capping does indeed play an important role in the control actin polymerization.

In these studies we have used rhodamine-labeled muscle actin (RA)[1] both in injection experiments to investigate the actin dynamics in intact cells and in a permeabilized cell assay to study the control of actin polymerization. Injection of derivatized actin has been used by a number of laboratories to study actin turnover in living cells (Kreis, 1986; Taylor and Wang, 1978). We have extended this line of investigation using quantitative fluorescence analysis. Our results provide independent evidence for centripetal flux of actin filaments in fibroblast lamellipodia. To investigate the control of actin polymerization in the absence of monomer sequestering we followed the incorporation of exogenous actin in permeabilized cells. This required developing a permeabilized cell assay which retained the essential features of spatial control of actin polymerization we observed in living cells. We have used this novel permeabilized cell assay to quantitate the extent and study the sites for actin polymerization in lamellipodia.

Materials and Methods

Preparation and Characterization of RA

Actin was prepared (Pardee and Spudich, 1982) from frozen rabbit muscle (Pel-Freez Biologicals, Rogers, AR) and stored, after freezing in liquid nitrogen, at 200 to 400 μM at −80°C in G-buffer (5 mM Tris-HCl, pH 8.7, 0.2 mM ATP, 0.2 mM $CaCl_2$, 0.02% 2-mercaptoethanol, and 0.02% sodium azide). This actin ran as a single 43-kD band during SDS-PAGE, showing that it is essentially free of contaminants. The actin was derivatized in the filamentous form with *N*-hydroxysuccinimidyl 5-carboxytetramethyl rhodamine (NHSR) (Molecular Probes Inc., Junction City, OR) as previously described (Kellogg et al., 1988). Two cycles of assembly–disassembly were performed. The final G-actin was dialyzed against injection buffer (1 mM Hepes, pH 7.5, 0.2 mM $MgCl_2$, and 0.2 mM ATP) for 4 h, clarified by centrifugation at 100,000 *g* in an airfuge (Beckman Instruments, Palo Alto, CA) for 10 min, frozen in aliquots in liquid nitrogen, and stored at −80°C. The stoichiometry was ~0.35 rhodamine molecules per actin monomer as determined by absorption spectrophotometry using an extinction coefficient ϵ_{280}=48,988 $M^{-1}cm^{-1}$ for actin (Houk and Ue, 1974) and ϵ_{560}=50,000 M^{-1} cm^{-1} for tetramethyl Rhodamine (Molecular Probes Inc.).

The use of NHSR muscle actin for the study of actin turnover has been documented previously (Kellogg et al., 1988). We extended this characterization and showed that this probe is well behaved in that it incorporates in all discernable actin structures of the microinjected fibroblasts and remains so over the course of several hours. Also, the overall kinetics of RA incorporation into the various actin cytoskeleton structures are similar to those previously observed using a variety of related probes (Amato and Taylor, 1986; Glacy, 1983; Kreis et al., 1979; Okabe and Hirokawa, 1989). Furthermore, when RA was injected in motile cells, no changes in cell behavior, such as lamellipodial protrusion and retraction, could be detected. Finally, although we only presented the data making use of RA, all the experiments discussed in this paper were reproduced using iodoacetamide-biotin-derivatized muscle actin. The latter was visualized using indirect immunofluorescence with anti-biotin antibodies. This probe labels cysteine 374 as opposed to lysine residues for the NHS-rhodamine label. Taken together these data suggest that derivatization of the actin does not significantly alter its dynamic properties in permeabilized or intact cells.

Denatured actin for microinjection was prepared by converting ATP-actin into ADP-actin by incubation with 20 U/ml hexokinase and 1 mM glucose. This actin completely lost its competence to polymerize after 24 h. Control injection of ATP-actin with hexokinase and glucose gave results indistinguishable from injection of ATP-actin alone.

1. *Abbreviations used in this paper*: OM, observation medium; NHSR, *N*-hydroxysuccinimidyl 5-carboxytetramethyl rhodamine; RA, rhodamine-labeled muscle actin.

Cell Culture

NIH-3T3 cells (kindly provided by Dr. D. Aghib, University of California, San Francisco, CA) were grown in MEM EBSS medium, supplemented with 5% FCS, penicillin, and streptomycin, at 37°C in 5% CO_2. Coverslips for microinjection and permeabilized cell experiments were coated with 2 mg/ml high molecular weight (>300 kD) poly-D-lysine (P1024; Sigma Chemical Co., St. Louis, MO) for ~1 h, rinsed with distilled water and air dried. Just before plating, the coverslips were incubated with Con A (3 μM, suspended in 10 mM MES, pH 6.0) for ~1 h and rinsed. Coverslips were used within 3 to 4 h after plating.

Microinjection and Staining

Just before microinjection coverslips were transferred to observation medium (OM): bicarbonate- and phenol-red-free MEM EBSS, buffered with 20 mM Hepes, pH 7.4, 5% FCS, penicillin, and streptomycin. Coverslips were then mounted in the same medium in a thermostatted chamber, keeping the cells at 37°C. The chamber was fixed to the stage of a microscope (model IM35; Zeiss, Oberkochen, Germany). An aliquot of RA was thawed, diluted with injection buffer to 50 μM, and clarified by centrifugation in the airfuge (Beckman Instruments) at 100,000 rpm for 20 min. Borosilicate injection needles (FHC, Brunswick, ME) were acid washed before use. Injections were performed using continuous flow and were done by inserting the needle in the perinuclear area. Cells were followed during injection and permeabilization using video microscopy. Time-lapse imaging was performed using the apparatus previously described (Sawin and Mitchison, 1991). Cells which showed any abnormal behavior during injection (i.e., retraction of lamellipodia) were not taken into account. The injected volume was estimated to be ~10% of total cell volume. Assuming the concentration of total cellular actin to be ~100 μM (Bray and Thomas, 1975), the concentration of RA in the cell would thus be only 5% of the total actin concentration. After variable incubation times the cells were simultaneously permeabilized and fixed for 10 min on the stage in cytoskeleton buffer (CB): 10 mM MES, pH 6.1, 138 mM KCl, 3 mM $MgCl_2$, and 2 mM EGTA, containing 0.5% Triton X-100 and 0.5% glutaraldehyde. This buffer was chosen for its superior preservation of actin filament structure on fixation (Small, 1981; Small, 1985). Cells were subsequently rinsed in TBS-TX (0.15 M NaCl, 0.02 M Tris-Cl, pH 7.4, containing 0.1% TX-100) and reduced with 1 mg/ml $NaBH_4$ in TBS, for 5 min, three times. The coverslips were rinsed in TBS-TX, and incubated for 20 min with FITC phalloidin (1 μg/ml dissolved in TBS-TX). The coverslips were thoroughly rinsed with TBS-TX and mounted in 70% vol/vol glycerol, 10 mM Tris-HCl, pH 8.2 to which 5 mg/ml diamino-benzene was added as an oxygen scavenger. The mounting medium was purged with nitrogen before adding diaminobenzene, and was stored in a sealed syringe at −20°C.

Permeabilized Cell Experiments

We optimized two parameters which appeared to be crucial for adequate preservation of the actin cytoskeleton during cell permeabilization: the adhesiveness of the substrate and the type and concentration of the detergent. We found that more adhesive substrates gave better preservation, which led to the development of the polylysine-Con A–coated glass substrate, described above. Since Con A is known to stimulate actin polymerization (Condeelis, 1979), the turnover of the actin cytoskeleton is likely to be quantitatively different from what could be observed on less adhesive substrates. However, an internal control is provided by the use of ratio imaging of incorporated rhodamine-actin over intrinsic phalloidin-stained filaments. With respect to the permeabilization conditions we found that cholesterol-chelating detergents, such as saponin, were far better than nonionic detergents such as Triton X-100 for preserving actin structures, as monitored by inspection of the phalloidin staining. The lowest concentration of saponin which allowed actin monomers to enter the permeabilized cells reproducibly was ~0.2 mg/ml.

To study actin incorporation in permeabilized cells, fibroblasts were plated on 18-mm^2 coverslips coated with polylysine-Con A. 15 min before the experiment the coverslips were transferred to OM at 37°C. At the start of the experiments a coverslip was transferred to a 35-mm petri dish, containing 1 ml of OM, and brought to room temperature (23°C) by putting the petri dish on a wet copper block for ~1 min. The following procedures were all performed at room temperature (we did not succeed in achieving adequate preservation of the cells using 37°C permeabilizations). The coverslip was briefly washed by dipping in rinsing buffer (RB): 20 mM Hepes, pH 7.5, 138 mM KCl, 4 mM $MgCl_2$, 3 mM EGTA. The coverslip was then

transferred, cell side up, to parafilm. All subsequent incubation media consisted of permeabilization buffer (RB plus 0.2 mg/ml saponin). All medium exchanges of the respective media (50 μl per coverslip) were performed by tilting the coverslip, adsorbing the medium with Whatman 3MM adsorbent paper on one side of the coverslip and gently adding the new medium at the other side of the slip, a process which took ~15 s per exchange. It was essential to perform the buffer changes gently to avoid damaging of lamellipodial structure. For every incubation with new medium, the medium exchange was repeated at least once to provide thorough exchange. A 100 μM stock solution of RA was rapidly thawed from −80°C, diluted typically 10-fold in injection buffer and sonicated using a vibracell sonicator (Sonics & Materials, Danbury, CT) provided with a micro tip. The RA suspension was clarified in a microfuge for 20 min, although generally no pellet could be observed after the sonication procedure. For the incubations with RA, 1 mM ATP was added to the incubation medium to permit efficient polymerization of the added actin. RA was added to this medium just before application to the cells. Under these conditions no extracellular filaments could be observed after fixation, indicating that filament nucleation occurred only from sites located in the permeabilized cells. If the sonication and centrifugation steps were omitted, actin filaments could be observed all over the entire coverslip. After incubation with RA the cells were fixed for 10 min in cytoskeleton buffer containing 0.5% glutaraldehyde and 0.2% Triton-TX. The coverslips were further processed as described for the microinjection experiments.

Fluorescence Microscopy

Fluorescence imaging and data collection was performed on an inverted microscope (Olympus Corporation of America, New Hyde Park, NY) and a Peltier-cooled CCD camera as previously described (Hiraoka, 1989). FITC–phalloidin and rhodamine fluorescence was imaged using high-performance fluorescein and Texas red filter sets (Omega Optical, Brattleboro, VT) to minimize bleedthrough. Two different CCD chips were used: a Kodak-Videc 1,340 × 1,037 pixel chip (Eastman Kodak Co., Rochester, NY), used in the bin-2 mode conjunctly with a 60×, 1.4 NA SPlanApo Olympus objective or a 512 × 512 pixel chip (Texas Instruments Inc., Dallas, TX) in conjunction with a 40×, 1.3 NA DApo Olympus objective. In this way the resolution was 0.15 μm/pixel. Color pictures were obtained using a Dunn digital camera and Ektachrome 200 slide film. For the black and white pictures we used Technical Pan film.

Data Analysis

To determine the density of the intrinsic actin cytoskeleton we made use of the quantitation of fluorescent phalloidin (Howard and Oresajo, 1985). Although some actin-binding proteins are known to compete with phalloidin for actin binding sites (Nishida et al., 1987), it is very unlikely that this would significantly bias the evaluation of actin filament density.

Images were displayed and manipulated using a program designed for analyzing three-dimensional optical data, PRISM (Chen et al., 1989). For the calculation of ratio images, each pair of fluorescein and Texas red images was checked for translation and magnification artefacts by aligning small specks (2–5 pixels wide) of fluorescence present in both channels. No significant magnification error between the fluorescein and Texas red channels could be detected in this way. Translation errors were minimal, at the most one pixel, and, if present, these deviations were taken into account. For the display of the ratio images we used a two-dimensional look-up table, consisting of 16 different hues and 16 grey levels, corresponding to the ratio and the sum of the intensities of the two images, respectively (Paddy et al., 1990).

Fluorescence quantitation was straightforward because of the large dynamic range (12 bits) and linearity of the CCD camera. Shading corrections were made as previously described (Hiraoka et al., 1989). Since we were mainly interested in quantitating fluorescence from the extremely thin (0.2 μm) lamellipodia and immediately adjacent areas making up the thin cytoplasmic veils, no removal of out-of-focus information was necessary. A motorized focussing mechanism allowed us to focus on lamellipodia to within 0.1 μm. To eliminate observer bias in the quantitation of RA incorporation, we used the following procedure: cells with well-preserved lamellipodia were first selected using the fluorescein channel alone. Subsequently, the fluorescein and the corresponding Texas red images were recorded and stored on a high-capacity optical disk (Emulex Corp., Costa Mesa, CA). Since examination and focussing was performed by means of the fluorescein image and because of the presence of an effective antibleach agent, bleaching of the rhodamine image was minimal. All the data from a given experiment were quantitated on the same day.

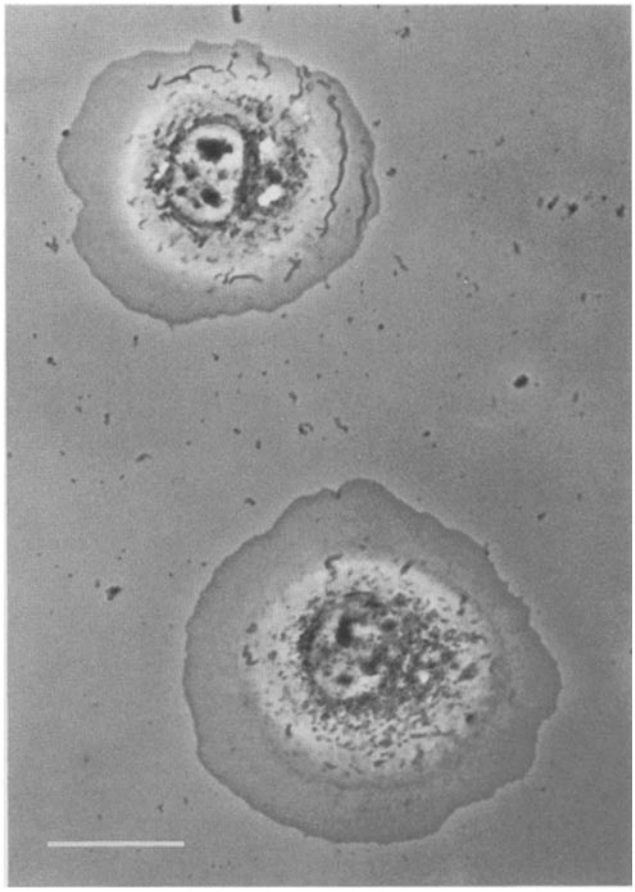

Figure 1. Phase contrast image of cells plated on polylysine/Con A-coated coverslips. Bar, 20 μm.

Quantitation of fluorescence for the permeabilized cell assays was done by measuring the average pixel intensity at the tips of lamellipodia selected by inspection of the fluorescein images. These regions were outlined with a mouse and were typically ~5 pixels across and 20–50 pixels wide. We found that most of the variance in the intensity data was contributed by differences between cells, rather than by differences between various lamellipodia of the same cell (not shown). Therefore, for each cell between one and four areas were selected, the intensities were averaged, and subsequently an average was made over the 10 to 20 cells which were recorded for each coverslip. Only flat lamellipodia were quantitated. Ruffling areas, which could easily be detected in the fluorescein channel, were not taken into account. No systematic differences could be detected between different areas of the coverslips. Since the variation between different coverslips prepared under the same conditions was minimal (5–10%) usually only one coverslip was quantitated per data point.

Results

Microinjected RA Incorporates at the Tip of Lamellipodia and Undergoes Subsequent Centripetal Transport

We studied the time course and localization of actin monomer incorporation into the cytoskeleton by microinjection of RA, followed by permeabilization/fixation of the cells after variable incubation times. We used NIH-3T3 fibroblasts within 4 h after plating on an adhesive substrate consisting of glass coverslips coated with polylysine and Con A. Compared to untreated glass, this procedure was found to improve dramatically the preservation of lamellipodia during

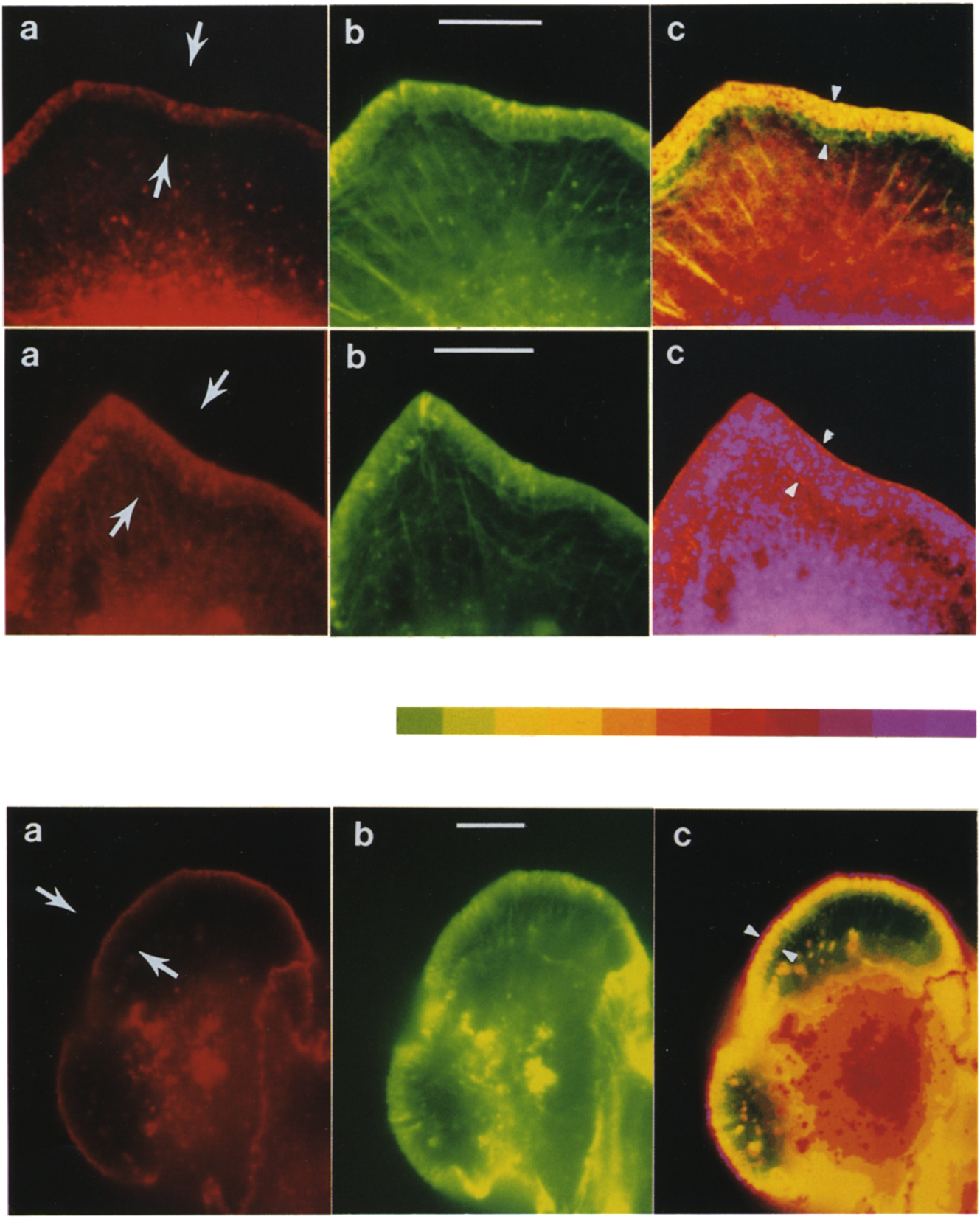
a
b
c
a
b
c
a
b
c

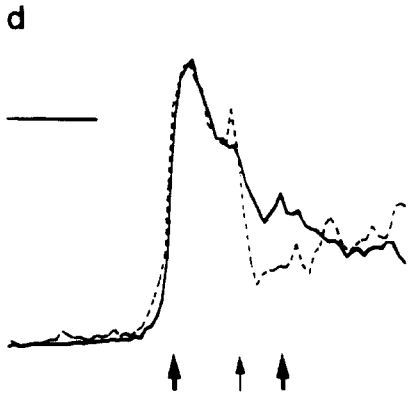

Figure 2. Localization of rhodamine-actin incorporation in fibroblasts fixed shortly after injection. (*a–c*) shows a detail of a cell simultaneously permeabilized and fixed 24 s after injection. (*a*) Rhodamine stain, showing newly incorporated actin. The arrows outline the section corresponding to the profiles in (*d*). (*b*) Fluorescein-phalloidin stain, showing both preexisting and newly incorporated filaments; (*c*) rhodamine/fluorescein ratio image, the arrowheads delineate the lamellipodium, and correspond to the fat arrows marked in the intensity profiles. The appearance of the stress fibers in the ratio image (*c*) as yellow over a red background, while they are not visible in the rhodamine image (*a*) itself, is caused by the higher background in the perinuclear part of the rhodamine image, which is divided by the stress fibers in the corresponding area of the fluorescein image (*b*). (*d*) Normalized intensity profiles from the respective channels along the lines delineated by arrows in *a*. (—) Fluorescein profile; (- - - -) rhodamine profile. The fat arrows in *d* delineate the lamellipodium, the thin arrow indicates the front of the wave of incorporated actin. See Materials and Methods for further details. The color scale from green to purple corresponds to low and high rhodamine/fluorescein ratios, respectively. Bars, (*b*) 10 μm; (*d*) 2.5 μm.

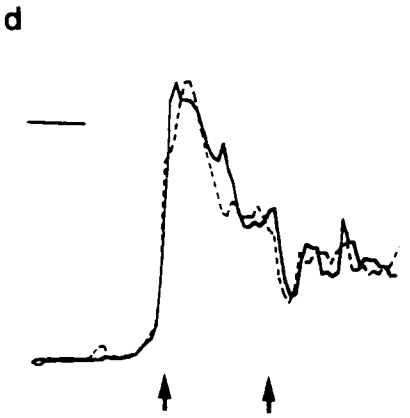

Figure 4. Steady-state incorporation of injected actin, showing a detail of a cell fixed 20 min after injection. (*a*) Rhodamine stain, showing the incorporated actin. The arrows outline the section corresponding to the profiles in *d*. (*b*) Phalloidin stain. (*c*) Rhodamine/fluorescein ratio image, arrowheads delineate the lamellipodium boundaries. (*d*) Normalized intensity profiles along the section marked in *a*. Full-line fluorescein profile and dashed line, rhodamine profile. Fat arrows delineate the lamellipodium. Bars: (*b*) 10 μm; (*d*) 2.5 μm.

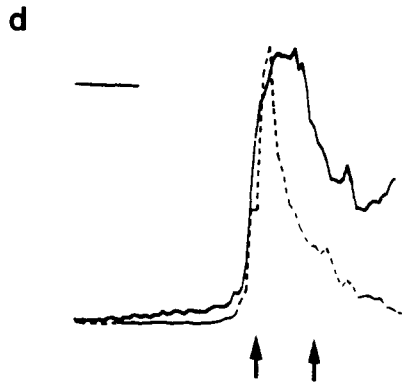

Figure 5. Rhodamine-actin incorporation in saponin-permeabilized cells. (*a*) rhodamine stain, showing exogenous actin incorporation; (*b*) fluorescein-phalloidin stain, showing preexisting and newly incorporated filaments; (*c*) rhodamine/fluorescein ratio, arrowheads outline the lamellipodial boundary; and (*d*) intensity profiles along the arrows shown in *a*. For this experiment 0.4 μM RA was added together with 0.2 mg/ml saponin in permeabilization buffer and incubated for 5 min before fixation. Bars: (*b*) 10 μm; (*d*) 2.5 μm.

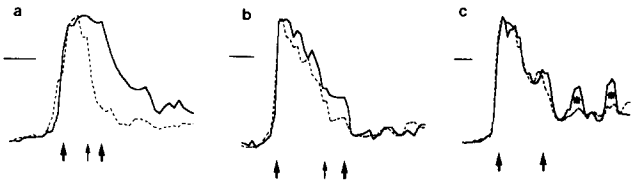

Figure 3. Normalized profiles of incorporated and intrinsic actin for various incubation times, (*a*) 14 s, (*b*) 22 s, and (*c*) 78 s. (—) fluorescein intensity profiles, corresponding to the intrinsic actin cytoskeleton; (- - - -) rhodamine intensity profiles, corresponding to the newly incorporated actin. The fat arrows delineate the lamellipodium, the thin arrows in *a* and *b* indicate the front of the wave of incorporated actin. Bars, 1 μm.

the permeabilization procedures described in the next section. Fibroblasts spread rapidly (15–30 min) on this substrate, typically adopting a roughly radially symmetric morphology (Fig. 1), and did not show any further changes in morphology until they slowly started polarizing ~5 h after plating. These highly spread cells displayed relatively broad (2–4 μm), actin-rich lamellipodia around most of their circumference (see for example Figs. 2 *b* and 3 *b*). Here, we define lamellipodia as those thin regions located at the cell periphery where the actin meshwork is much more dense than in the remainder of the cell (Vasiliev, 1991). On less adhesive substrates, these lamellipodia continuously retract and protrude. On the highly adhesive substrate lamellipodial retraction and protrusion was strongly inhibited during the first few hours after plating. Stress fibers were usually poorly developed under these conditions.

An example of a cell fixed 24 s after injection is shown in Fig. 2, *a–d*. The injected RA preferentially incorporated in the outer part of the lamellipodium (compare Fig. 2, *a* and *b*). To relate the amount and distribution of the incorporated actin with respect to the intrinsic actin we calculated the ratio of the rhodamine over the fluorescein image and applied a two-dimensional pseudo-color look-up table (see Materials and Methods). The result is depicted in Fig. 2 *c* in which the lamellipodium is outlined by arrowheads, showing that the band of incorporated actin (yellow–orange) is restricted to the front of the lamellipodium. The base of the lamellipodium appears green in the ratio image, indicating that subunit incorporation was much less extensive in this area. The distribution of RA incorporation is also evident from a comparison of the rhodamine- and fluorescein-intensity profiles. These profiles were measured along the arrows in Fig. 2 *a* and are shown in Fig. 2 *d*. The intensity of rhodamine and fluorescein fluorescence is similar in the distal region of the lamellipodium which incorporated RA (delineated by the *thin arrow* in Fig. 2 *d*), whereas in the proximal region, the rhodamine intensity is significantly lower. It should be noted here that, especially in cells fixed very shortly after injection, there is a diffuse rhodamine staining visible in the perinuclear region (see Fig. 2 *a* and compare the rhodamine and fluorescein profiles in Fig. 2 *d*), which makes ratio imaging difficult in the thicker areas of the cytoplasm. This perinuclear staining is probably caused for a larger part by trapping RA monomers during the fixation procedure (see below). The lamellipodial rhodamine staining, however, is predominantly if not exclusively caused by polymerized RA, since upon injection of denatured ADP-actin we could not detect any significant actin incorporation in the lamellipodia (<10% of the controls).

The gradual incorporation of injected RA in lamellipodia is further illustrated in Fig. 3, showing the fluorescence intensity profiles along sections in three cells fixed 14, 22, and 78 s after injection. All cells fixed within 30 s after injection showed a discrete band of incorporated actin which started at the edges, but did not fill the entire lamellipodium (Fig. 3, *a* and *b*). Cells fixed after longer incubation times incorporated RA across the whole lamellipodium (Fig. 3 *c*).

10–20 min after injection, the rhodamine image was essentially identical to that of fluorescein. The homogeneous incorporation of the injected actin into the preexisting structures is evident from the uniform color in the ratio image (Fig. 4 *c*), as well as from inspection of the rhodamine- and fluorescein-intensity profiles across the lamellipodium (Fig. 4 *d*).

The relatively high background of RA in the thicker areas of the injected cells makes it very difficult to evaluate the turnover of the cortical cytoskeleton using this method. Stress fibers took considerably longer than lamellipodia to turn over. For example, very little incorporation could be seen after 78 s of incubation (Fig. 3 *c*, *asterisks*), whereas homogeneous incorporation was evident after 20 min (Fig. 4). Similarly slow turnover rates have been reported in a variety of other studies (Amato and Taylor, 1986; Glacy, 1983; Kreis et al., 1979; Okabe and Hirokawa, 1989).

Incorporation of RA in Saponin-permeabilized Fibroblasts Is Limited to A Narrow Region at the Tip of Lamellipodia

While our microinjection experiments provide useful information about the spatial organization of actin dynamics, they cannot address the underlying molecular mechanisms. In particular we could not distinguish whether selective polymerization at the distal edge of the lamellipodium was because of local desequestration of subunits, local availability of nucleation sites, or both. To bypass monomer sequestration, we designed an assay to study the spatial control of exogenous actin polymerization in permeabilized cells. The considerations that went into the development of the permeabilization conditions are mentioned in Materials and Methods. Fibroblasts were permeabilized in the presence of rhodamine-labeled actin monomers and after 5 min were fixed and stained with fluorescein–phalloidin to visualize all actin filaments. A typical cell with well-preserved lamellipodia is shown in Fig. 5. RA incorporation was observed within a narrow strip at the distal end of the lamellipodia (Fig. 5, *a* and *b*). The ratio image confirmed that the region of RA incorporation was located at the very tip of these lamellipodia (Fig. 5 *c*). The rhodamine-intensity profile (Fig. 5 *d*), outlined by the arrows in Fig. 5 *a*, showed that the width of the incorporated band (at half the maximum intensity) was ~1 μm for this cell. The average width of the incorporated RA band varied between preparations, but was always smaller than the width of the preexisting lamellipodium. The rhodamine staining at the tips of lamellipodia is because of polymerized RA, since it is strongly inhibited by CapZ (see below) or cytochalasin D (not shown), whereas the perinuclear stain is not. Less well-preserved lamellipodia appeared to be withdrawn and incorporated RA throughout most of their width.

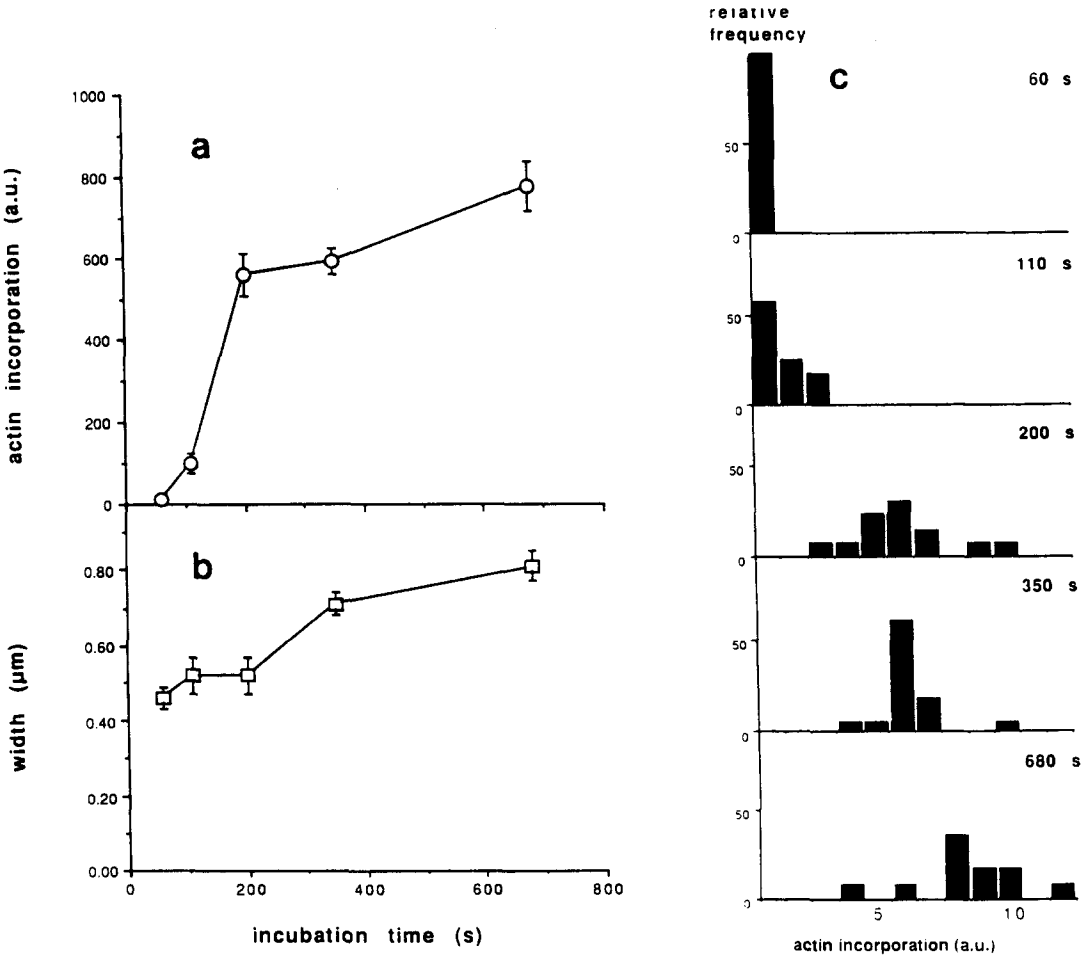

Figure 6. Kinetics of rhodamine-actin incorporation in permeabilized cells. (*a*) Extent of the incorporated actin, see Methods for details of the measurement. Averages and SEM of at least 10 different cells. (*b*) Width of the incorporated area as a function of the incubation time, measured from intensity profiles across the lamellipodia as the width of the band at half-maximum intensity. Averages and SEM of at least 10 different cells. (*c*) Histograms illustrating the distribution of the extent of actin incorporation for the different incubation times corresponding to the data points in *a* and *b*. The incubation times are indicated in each histogram. 0.4 μM RA was added to the permeabilization medium containing 0.2 mg/ml saponin and incubated for the time indicated.

It is clear from both the ratio image (Fig. 5 *c*) and the respective fluorescence profiles (Fig. 5 *d*) that the RA background staining in the cytoplasm just behind the lamellipodium is much less pronounced than in the case of the injected cells (Fig. 2). This is presumably because a substantial amount of cytoplasmic protein is extracted by permeabilization, diminishing the trapping of RA monomers during fixation. Rhodamine/fluorescein ratio imaging of RA incorporation in the permeabilized cells thus shows that with respect to the incorporation of actin at the tips of lamellipodia, actin incorporation into the cytoskeleton adjacent to the lamellipodia is strongly inhibited.

To study the kinetics of actin incorporation in the permeabilized cells the average rhodamine intensity at the tips of lamellipodia was quantitated using a cooled CCD camera as described in Materials and Methods. The extent of incorporation was plotted as a function of the incubation time, as shown in Fig. 6 *a*, while the width of the band of incorporated actin as a function of time, is shown in Fig. 6 *b*. Actin incorporation appeared to have a lag time of 30 to 60 s and started to level off after ~3 min of incubation time. To determine whether the time course of RA incorporation reflected the polymerization rate or the permeabilization kinetics, we inspected the cell-to-cell variation of the RA incorporation. Fig. 6 *c* clearly shows a gradual and homogeneous increase of the rhodamine intensity at the edges of lamellipodia in time, indicating that it took ~1 min for the saponin to make large enough holes in the plasma membrane to allow for the passage of actin monomers and that further permeabilization is not the limiting factor determining the overall kinetics of RA incorporation. The average width of the incorporated RA band approximately doubled over the whole time course, but remained <1 μm in this set of experiments, even after incubation times up to 10 min.

Actin Nucleation in Permeabilized Fibroblasts Occurs at Barbed Endlike Structures

To obtain more information concerning the nature of the sites responsible for actin nucleation in lamellipodia we performed two experiments which allowed us to distinguish between barbed- and pointed- end subunit addition. First, we looked at the effect of CapZ, a protein which specifically caps the barbed end of actin filaments (Caldwell et al., 1989)

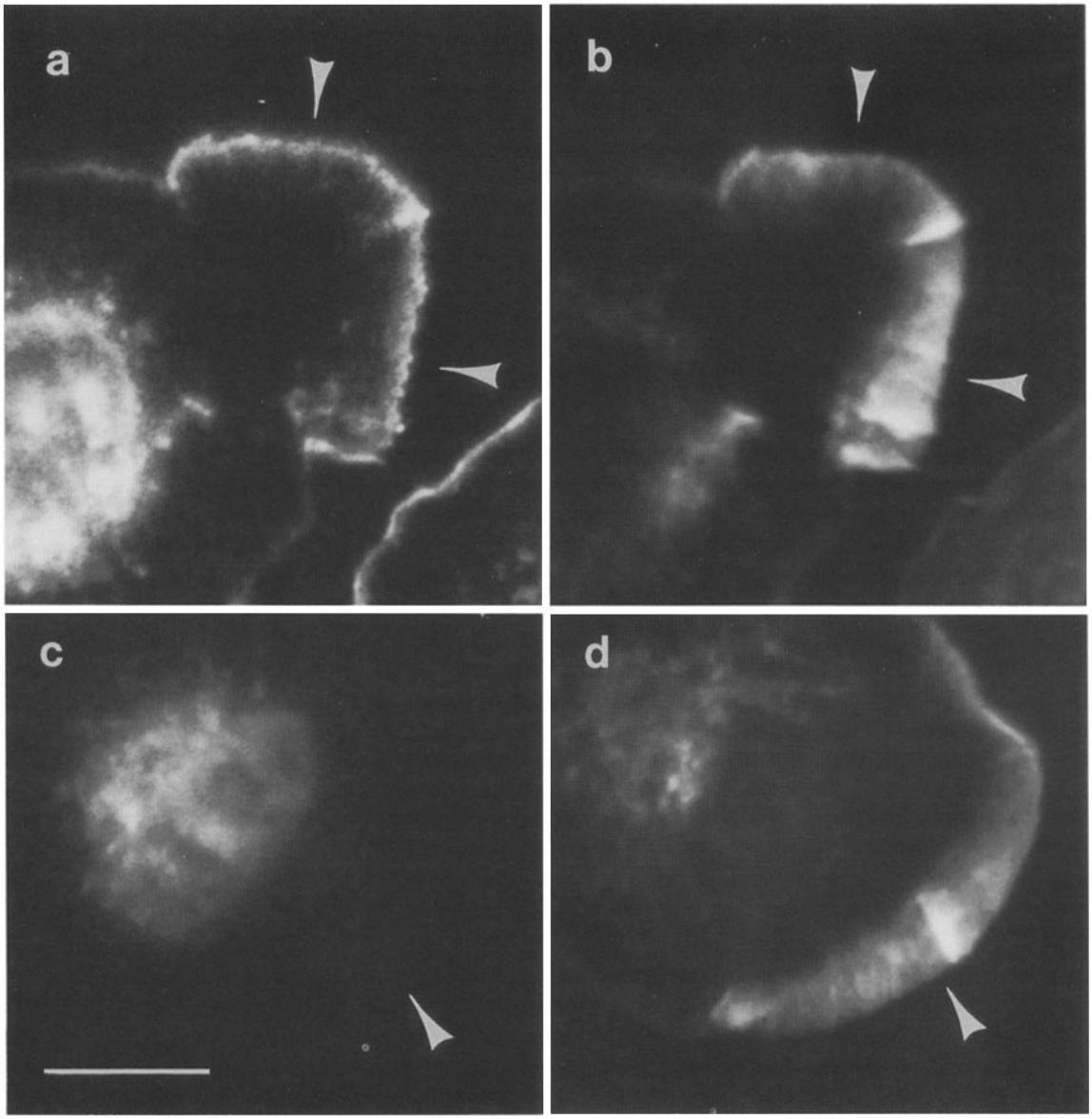

Figure 7. Inhibition of rhodamine-actin incorporation in permeabilized fibroblasts by CapZ. (*a* and *b*) cells were permeabilized in the presence of 1 μg/ml of fluorescein-phalloidin for 2 min, rinsed three times with permeabilization buffer over the course of 2 min, and subsequently incubated for 4 min with 0.4 μM rhodamine-actin in permeabilization buffer. (*a*) Rhodamine, and (*b*) fluorescein-phalloidin stain. (*c* and *d*) Rhodamine and fluorescein-phalloidin stain, respectively, of a cell incubated with RA in the presence of CapZ. Conditions as for *a* and *b* except that 20 nM CapZ was present throughout the whole experiment. Arrowheads indicate well-preserved lamellipodia. The part of the cell included at the right hand/bottom of *a* and *b* has a very narrow, partly ruffling lamellipodium, and shows a relatively high RA incorporation. Bar, 10 μm.

and second, we determined the critical concentration of the RA incorporation. For the latter experiment we wanted to eliminate as much as possible, any contributions from the intrinsic monomeric actin pool. We therefore permeabilized the cells in the presence of FITC-phalloidin for 90 s to stabilize the intrinsic actin filaments, and subsequently rinsed the coverslips with permeabilization buffer (in the absence of phalloidin) multiple times during 2 min to remove both actin monomers and unbound phalloidin, and only then applied the RA-containing buffer. Without phalloidin stabilization of the intrinsic actin cytoskeleton lamellipodial actin content and the degree of preservation severely decreased after repeated exchanges of the medium (not shown).

CapZ, a protein purified from the Z-band of muscle, was shown to specifically cap the barbed end of actin filaments, with a Kd of about 0.5 nM. It does not bind to actin monomers at all (Caldwell et al., 1989). CapZ has also been shown to nucleate actin, but at the concentrations of actin used in our assay (<1 μM), this effect should be negligible (Caldwell et al., 1989). As can be seen in Fig. 7, RA incorporation in lamellipodia is strongly inhibited by the presence of 20 nM CapZ, compare Fig. 7, *a* and *c*, while the density of the intrinsic actin making up the cytoskeleton of the lamellipodia is much less affected, compare Fig. 7, *b* and *d*. In CapZ titration experiments we observed that the half-maximal concentration for inhibition of actin incorporation was

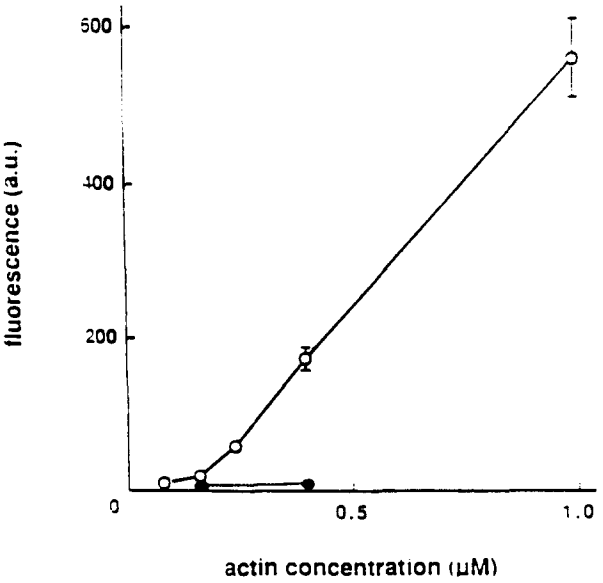

Figure 8. Concentration dependence of rhodamine-actin incorporation. Experimental procedures were as in Fig. 7, except that the RA concentration was varied as indicated. (○) No CapZ was present; (●) 20 nM CapZ was present throughout the whole experiment. Averages and SE of typically 10–20 cells.

~2 nM (not shown), which is close to the Kd for barbed end binding obtained in vitro. Quantification of the rhodamine tip staining showed that for a RA concentration of 0.4 μM and a CapZ concentration of 20 nM, actin incorporation is inhibited by 95%. The fluorescein-phalloidin stain is inhibited by <30%, indicating that the intrinsic filaments are relatively stable under these conditions. The perinuclear rhodamine staining is inhibited by only 40% under the same conditions, indicating that this staining for the larger part does not reflect barbed-end incorporation. The presence of the perinuclear stain at RA concentrations below the pointed end critical concentration, which is ~0.6 μM (Pollard, 1986), indicates furthermore that it is not caused by incorporation from pointed ends either. Thus, it is likely to be mainly because of monomer trapped during fixation.

The concentration dependence of the RA incorporation is shown in Fig. 8. Specific RA staining could be observed after incubation with concentrations above 0.15 μM, which is close to the critical concentration of actin polymerization in vitro (Pollard, 1986). This concentration is definitely lower than the critical concentration for monomer addition to the pointed end of microfilaments, showing, in agreement with the CapZ inhibition studies, that the nucleation sites for actin polymerization at the tip of lamellipodia resemble the barbed ends of actin filaments.

Discussion

Turnover of Actin in Live Cells

In this paper we have used fluorescently derivatized actin to study the sites and control of actin polymerization in both live and permeabilized fibroblasts. Ratio imaging (Taylor et al., 1986) of recently polymerized versus total actin showed that the injected RA incorporates initially at the front of lamellipodia and after ~30 s fills the whole lamellipodium. Together with the observation that in permeabilized cells actin incorporation is restricted to within 0.5 to 1 μm from the tips of lamellipodia, these results provide independent evidence for a model in which actin continuously polymerizes at the tip followed by centripetal flux of the polymerized actin, in qualitative agreement with a number of other reports (Forscher and Smith, 1988; Svitkina et al., 1986; Wang, 1985). We measured the speed of this centripetal flux by dividing the width of the incorporated actin band by the time between injection and fixation, yielding an average of 4.5 ± 0.3 (SEM) μm/min, estimated from nine different lamellipodia from five different cells. As we do not know the time it takes for the monomer to diffuse from the site of injection to the lamellipodium, this value only determines a lower boundary for the flux rate, which could be as high as 10 μm/min. The rate of the centripetal flux we can extrapolate from our experiments is thus in the range of centripetal flux measurements published in the literature for fibroblasts and neuronal growth cones using video-enhanced differential interference contrast (Fisher et al., 1988; Forscher and Smith, 1988). This rate, however, is about an order of magnitude faster than that obtained in photobleaching experiments (Wang, 1985), as well as the rate which we have estimated from published data on microinjection of biotinylated actin (Okabe and Hirokawa, 1989). Since in living cells the centripetal flux of actin is at least 5 μm/min, our observation that in the permeabilized cells the incorporation is limited to the distal tip of the lamellipodia indicates that this in vivo flux ceases within one minute or less after permeabilization.

The observations of centripetal flux of polymerized actin in lamellipodia raise the question as to where the actin filaments depolymerize. Since frequently (Fig. 2, *b* and *f*), no significant accumulation of F-actin can be seen at the base of lamellipodia, most of the actin has to depolymerize before or at the time it reaches the base of these lamellipodia. In addition, almost all lamellipodia we inspected, displayed a decreasing gradient of actin density, tip to base (Fig. 2, *d* and *h*; Fig. 3, *b* and *c*; and Fig. 4 *d*). These gradients were observed in injected as well as in control cells. We also observed similar gradients in the lamellipodia of cells plated on untreated glass. Together with the centripetal flux, this gradient indicates that disassembly of the actin cytoskeleton occurs throughout most of the width of the lamellipodia, as opposed to just at the base.

Characterization of the Actin Nucleation Sites in Permeabilized Fibroblasts

To study the spatial control of actin polymerization we developed a permeabilized cell system in which the actin cytoskeleton could be adequately preserved. Permeabilized cell systems used to study the control of the actin cytoskeleton have been described before (Carson et al., 1986; Hall et al., 1989; Hartwig and Janmey, 1989; Kreis, 1986; Sanger et al., 1984; Southwick et al., 1989). The uniqueness of the present assay lies in the high degree of preservation of the intrinsic cytoskeleton and hence its ability to yield information about the spatial control of actin polymerization. Furthermore, the same probe and cells can be used to study the control of actin nucleation and to follow actin dynamics in intact cells.

In well-preserved cells, incorporation of RA was restricted to the tips of lamellipodia. The RA incorporation at the tips of well-preserved lamellipodia appears to be highly

specific for several reasons: it is limited to within 1 μm from the tip of lamellipodia and is strongly inhibited by CapZ. What have we learned about the nature of the nucleating sites at the tips of lamellipodia? The critical concentration for monomer addition and the inhibition by CapZ indicate that these sites are made up of free barbed ends of actin filaments. These filaments could be part of the preexisting cytoskeleton or may be initiated by de novo nucleation sites. We have not thus far succeeded in discriminating between these possibilities. In addition, we cannot exclude the possibility that at higher concentrations of monomeric RA (>1 μM) free pointed ends start to contribute to the actin incorporation. However, because of their much higher critical concentration and slower polymerization rate, it is unlikely that free pointed ends play a significant role in cellular actin polymerization.

Control of Actin Nucleation in Fibroblasts

Essentially two mechanisms could contribute to the restriction of actin polymerization to the tips of lamellipodia in living cells: local release of monomers from sequestering proteins and/or local control of the accessibility of filament ends by a selective capping mechanism. The use of rhodamine-labeled muscle actin as an exogenous probe in the permeabilized fibroblasts ensures us that in this assay we can effectively bypass the putative monomer sequestering mechanisms. Indeed, it has been shown that injected muscle actin takes a considerable time, in the order of minutes, before most of it becomes sequestered (Sanders and Wang, 1990). This makes it extremely unlikely that, in the very short time between entering the permeabilized cell and incorporating into the cytoskeleton, RA would get sequestered by the cellular complement of G-actin–binding proteins. Thus, the observed selective RA incorporation at the tips of lamellipodia, in both permeabilized and live cells, shows that there is a relatively high concentration of uncapped filament ends or other nucleating entities in this area of the cell.

This very inhomogeneous distribution of free barbed ends in the cell could be created by two different mechanisms. Firstly, filament length could be essentially uniform in the cell. In this case the localized RA incorporation would imply that actin polymerization is governed by a spatially regulated capping activity, preferentially capping all the filaments in the cell except at the tips of the lamellipodia. Secondly, all the barbed ends in the cell could be free. In this case the density of the ends would result from the inhomogeneous distribution of filament length, with the lamellipodial tips having especially short filaments. Although the question of the length of lamellipodial, cortical, and stress fiber actin filaments has been addressed at the electron microscope level (Hartwig and Shevlin, 1986; Small, 1988), there is little agreement on the interpretation of the results. Filament length has also been assessed biochemically based on actin filament depolymerization kinetics in Dictyostelium discoideum (Podolski and Steck, 1990). This analysis suggested that a substantial degree of inhomogeneity in filament length could exist although no information on the spatial distribution of this inhomogeneity could be obtained. Relevant spatial information however, could be extracted from similar studies on neutrophils, showing that the average length of actin filaments was the same before and after activation (Cano, M., personal communication). This indicates that the distribution of actin filaments in lamellipodia (induced by activation) is similar to that in the cortex. We therefore favor the first hypothesis. We interprete our observations of preferential incorporation of actin at the tips of lamellipodia as demonstrating the existence of a regulated capping activity that allows subunit addition at the tips of lamellipodia and slows down the polymerization of actin elsewhere in the cell. This conclusion however, does not exclude the possibility that local desequestration of actin monomers also contributes to the spatial regulation of actin polymerization in vivo.

We are greatly indebted to J. Sedat and D. Agard (Howard Hughes Medical Institute, University of California, San Francisco, CA) for the use of their light microscope system and for enlightening discussions. We are also grateful to H. Chen, Z. Kam, M. Paddy, and J. Swedlow for advice and help with data analysis and to L. Reichardt (Howard Hughes Medical Institute, University of California, San Francisco) for frequent use of his imaging system. We wish to thank K. Miller and C. Fields for introducing us to the art of actin preparations. We also thank D. Aghib for a gift of NIH-3T3 cells and wish to express particular gratitude to J. Cooper (Washington University, St. Louis, MO) for a gift of CapZ and valuable discussion. We are most grateful to M. Cano, D. Lauffenburger, and S. Zigmond for sharing unpublished data with us. We also like to thank E. Bearer, B. Gumbiner, G. Pruliere, R. Ruggieri, K. Sawin, J. Theriot, and P. Wilson for critical reading of the manuscript.

This work was supported by National Institutes of Health grant (GM-39565) to T. J. Mitchison and Fellowships from the Packard Foundation and the Searle Foundation to T. J. Mitchison.

Received for publication 9 January 1991 and in revised form 22 April 1991.

References

Amato, P. A., and D. L. Taylor. 1986. Probing the mechanism of incorporation of fluorescently labeled actin in stress fibers. *J. Cell Biol.* 102:1074–1084.

Bray, D., and C. Thomas. 1975. The actin content of fibroblasts. *Biochem. J.* 147:221–228.

Buendia, B., M.-H. Bre, and E. Karsenti. 1990. Cytoskeletal control of centrioles movement during the establishment of polarity in Madin-Darby canine kidney cells. *J. Cell Biol.* 110:1123–1135.

Caldwell, J. E., S. G. Heiss, V. Mermall, and J. A. Cooper. 1989. Effects of CapZ, an actin capping protein of muscle, on the polymerization of actin. *Biochemistry.* 28:8506–8513.

Carson, M., A. Weber, and S. Zigmond. 1986. An actin-nucleating activity in polymorphonuclear leukocytes is modulated by chemotactic peptides. *J. Cell Biol.* 103:2707–2714.

Chen, H., J. W. Sedat, and D. A. Agard. 1989. Manipulation, display and analysis of three-dimensional biological images. *In* The Handbook of Biological Confocal Microscopy. J. Pawley, editor. IMR Press, Madison, WI. 127–135.

Condeelis, J. 1979. Isolation of concanavalin A caps during various stages of formation and their association with actin and myosin. *J. Cell Biol.* 80:751–758.

Condeelis, J., A. Hall, A. Bresnick, V. Warren, R. Hock, H. Bennett, and S. Ogihara. 1988. Actin polymerization and pseudopod extension during amoeboid chemotaxis. *Cell Motil. Cytoskeleton.* 10:77–90.

Fisher, G. W., P. A. Conrad, R. L. DeBiasio, and D. L. Taylor. 1988. Centripetal transport of cytoplasm actin, and the cell surface in lamellipodia of fibroblasts. *Cell Motil. Cytoskeleton.* 11:235–247.

Forscher, P., and S. J. Smith. 1988. Actions of cytochalasins on the organization of actin filaments and microtubules in a neuronal growth cone. *J. Cell Biol.* 107:1505–1516.

Glacy, S. D. 1983. Pattern and time course of rhodamine-actin incorporation in cardiac myocytes. *J. Cell Biol.* 96:1164–1167.

Hall, A. L., V. Warren, S. Dharmawardhane, and J. Condeelis. 1989. Identification of actin nucleating activity and polymerization inhibitor in ameboid cells: their regulation by chemotactic stimulation. *J. Cell Biol.* 109:2207–2213.

Hartwig, J. H., and P. Shevlin. 1986. The architecture of actin filaments and the ultrastructural location of actin-binding protein in the periphery of lung macrophages. *J. Cell Biol.* 103:1007–1028.

Hartwig, J. H., and P. A. Janmey. 1989. Stimulation of a calcium-dependent actin nucleation activity by phorbol 12-myristate 13-acetate in rabbit macrophage cytoskeletons. *Biochim. Biophys. Acta.* 1010:64–71.

Hiraoka, Y., J. S. Minden, J. R. Swedlow, J. W. Sedat, and D. A. Agard. 1989. Focal points for chromosome condensation and decondensation re-

vealed by three-dimensional in vivo time-lapse microscopy. *Nature (Lond.)*. 342:293–296.

Houk, T. W., and K. Ue. 1974. The measurement of actin concentration in solution: a comparison of methods. *Anal. Biochem.* 62:66–74.

Howard, T. H., and C. O. Oresajo. 1985. The kinetics of chemotactic peptide-induced change in F-actin content, F-actin distribution and the shape of neutrophils. *J. Cell Biol.* 101:1078–1085.

Kellogg, D. R., T. J. Mitchison, and B. M. Alberts. 1988. Behaviour of microtubules and actin filaments in living Drosophila embryos. *Development.* 103:675–686.

Kreis, T. E. 1986. Preparation, assay, and microinjection of fluorescently labeled cytoskeletal proteins: actin, a-actinin, and vinculin. *Meth. Enzymol.* 134:507–519.

Kreis, T. E., K. H. Winterhalter, and W. Birchmeier. 1979. In vivo distribution and turnover of fluorescently labeled actin microinjected into human fibroblasts. *Proc. Natl. Acad. Sci. USA.* 76:3814–3818.

Kreis, T. E., B. Geiger, and J. Schlessinger. 1982. Mobility of microinjected rhodamine actin within living chicken gizzard cells determined by fluorescence photobleaching recovery. *Cell.* 29:835–845.

Letourneau, P. C., T. A. Shattuck, and A. H. Ressler. 1987. "Pull" and "push" in neurite elongation: Observations on the effects of different concentrations of cytochalasin B and taxol. *Cell Motil. Cytoskeleton.* 8:193–209.

Mitchison, T., and M. Kirschner. 1988. Cytoskeletal dynamics and nerve growth. *Neuron.* 1:761–772.

Nishida, E., K. Iida, N. Yonezawa, S. Koyasu, I. Yahara, and H. Sakai. 1987. Cofilin is a component of intranuclear and cytoplasmic actin rods induced in cultured cells. *Proc. Natl. Acad. Sci. USA.* 84:5262–5266.

Okabe, R., and N. Hirokawa. 1989. Incorporation and turnover of biotin-labeled actin microinjected into fibroblastic cells: an immunoelectron microscopic study. *J. Cell Biol.* 109:1581–1595.

Omann, G. M., R. A. Allen, G. M. Bokoch, R. G. Painter, A. E. Traynor, and L. A. Sklar. 1987. Signal transduction and cytoskeletal activation in the neutrophil. *Physiol. Rev.* 67:285–322.

Paddy, M. R., A. S. Belmont, H. Saumweber, D. A. Agard, and J. W. Sedat. 1990. Interphase nuclear envelope lamins form a discontinuous network that interacts with only a fraction of the chromatin in the nuclear periphery. *Cell.* 62:89–106.

Pardee, J. D., and J. A. Spudich. 1982. Purification of muscle actin. *Methods Enzymol.* 85:164–181.

Podolski, J. L., and T. L. Steck. 1990. Length distribution of F-actin in Dictyostelium discoidium. *J. Biol. Chem.* 265:1312–1318.

Pollard, T. D. 1986. Rate constants for the reactions of ATP- and ADP-actin with the ends of actin filaments. *J. Cell Biol.* 103:2747–2754.

Pollard, T. D., and J. A. Cooper. 1986. Actin and actin-binding proteins: a critical evaluation of mechanisms and functions. *Annu. Rev. Biochem.* 55:987–1035.

Sanders, M. C., and Y.-L. Wang. 1990. Exogenous nucleation sites fail to induce detectable polymerization of actin in living cells. *J. Cell Biol.* 110:359–365.

Sanger, J. W., B. Mittal, and J. M. Sanger. 1984. Interaction of fluorescently labeled contractile proteins with the cytoskeleton in cell models. *J. Cell Biol.* 99:918–928.

Sawin, K. E., and T. J. Mitchison. 1991. Mitotic spindle assembly by two different pathways in vitro. *J. Cell Biol.* 112:925–940.

Small, J. V. 1981. Organization of actin in the leading edge of cultured cells: influence of osmium tetroxide and dehydration on the ultrastructure of actin meshworks. *J. Cell Biol.* 91:695–705.

Small, J. V. 1985. Factors affecting the integrity of actin networks in cultured cells. *In* Cell Motility: Mechanism and Regulation. H. Ishikawa, S. Hatano, and H. Sato, editors. University of Tokyo Press, Tokyo. 493–506.

Small, J. V. 1988. The actin cytoskeleton. *Electron Microsc. Rev.* 1:155–174.

Smith, S. J. 1988. Neuronal cytomechanics: the actin-based motility of growth cones. *Science (Wash. DC).* 242:708–715.

Southwick, F. S., G. A. Dabiri, M. Paschetto, and S. H. Zigmond. 1989. Polymorphonuclear leukocyte adherence induces actin polymerization by a transduction pathway which differs from that used by chemoattractants. *J. Cell Biol.* 109:1561–1569.

Stossel, T. P. 1989. From signal to pseudopod: how cells control cytoplasmic actin assembly. *J. Biol. Chem.* 264:18261–18264.

Stossel, T. P., C. Chaponnier, R. M. Ezzell, J. H. Hartwig, P. A. Janmey, D. J. Kwiatkowski, S. E. Lind, D. B. Smith, F. S. Southwick, H. L. Yin, and K. S. Zaner. 1985. Nonmuscle actin-binding proteins. *Ann. Rev. Cell Biol.* 1:353–402.

Svitkina, T. M., A. A. Neyfakh, and A. Bershadsky. 1986. Actin cytoskeleton of spread fibroblasts appears to assemble at the cell edge. *J. Cell Sci.* 82:235–248.

Taylor, D. L., and Y.-L. Wang. 1978. Molecular cytochemistry: incorporation of fluorescently labeled actin into living cells. *Proc. Natl. Acad. Sci. USA.* 75:857–861.

Taylor, D. L., P. A. Amato, P. L. McNeil, K. Luby-Phelps, and L. Tanasugarn. 1986. Spatial and temporal dynamics of specific molecules and ions in living cells. *In* Applications of Fluorescence in the Biomedical Sciences. Taylor, D. L., A. S. Waggoner, R. F. Murphy, F. Lanni, and R. R. Birge, editors. Alan R. Liss, Inc., NY. 347–376.

Vasiliev, J. M. 1991. Polarization of pseudopodial activities: cytoskeletal mechanisms. *J. Cell Sci.* 98:1–4.

Wang, Y.-L. 1985. Exchange of actin subunits at the leading edge of living fibroblasts: possible role of treadmilling. *J. Cell Biol.* 101:597–602.